

On the Use of Small Solar Panels and Small Batteries to Reduce the RAN Carbon Footprint

Original

On the Use of Small Solar Panels and Small Batteries to Reduce the RAN Carbon Footprint / Couto Da Silva, A.P., Renga, D., Meo, M., Ajmone Marsan, M.. - (2020), pp. 1-8. (2020 Mediterranean Communication and Computer Networking Conference, MedComNet 2020 ita 2020) [10.1109/MedComNet49392.2020.9191516].

Availability:

This version is available at: 11583/2853819 since: 2021-01-28T14:46:24Z

Publisher:

Institute of Electrical and Electronics Engineers Inc.

Published

DOI:10.1109/MedComNet49392.2020.9191516

Terms of use:

This article is made available under terms and conditions as specified in the corresponding bibliographic description in the repository

Publisher copyright

IEEE postprint/Author's Accepted Manuscript

©2020 IEEE. Personal use of this material is permitted. Permission from IEEE must be obtained for all other uses, in any current or future media, including reprinting/republishing this material for advertising or promotional purposes, creating new collecting works, for resale or lists, or reuse of any copyrighted component of this work in other works.

(Article begins on next page)

On the Use of Small Solar Panels and Small Batteries to Reduce the RAN Carbon Footprint

Ana Paula Couto da Silva¹, Daniela Renga², Michela Meo², Marco Ajmone Marsan^{2,3}

1 - Computer Science Department, Universidade Federal de Minas Gerais - Brazil

2 - Electronics and Telecommunications Department, Politecnico di Torino - Italy

3 - IMDEA Networks Institute - Spain

ana.coutosilva@dcc.ufmg.br, daniela.renga@polito.it, michela.meo@polito.it, marco.ajmone@polito.it

Abstract—The limited power requirements of new generations of base stations make the use of renewable energy sources, solar in particular, extremely attractive for mobile network operators. Exploiting solar energy implies a reduction of the network operation cost as well as of the carbon footprint of radio access networks. However, previous research works indicate that the area of the solar panels that are necessary to power a standard macro base station (BS) is large, making the solar panel deployment problematic, especially within urban areas.

In this paper we use a modeling approach based on Markov reward processes to investigate the possibility of combining a connection to the power grid with small area solar panels and small batteries to run a macro base station. By so doing, it is possible to exploit a significant fraction of renewable energy to run a radio access network, while also reducing the cost incurred by the network operator to power its base stations. We assume that energy is drawn from the power grid only when needed to keep the BS operational, or during the night, which corresponds to the period with lowest electricity price. The proposed energy management policies have advantages in terms of both cost and carbon footprint. Our results show that solar panels of the order of 1-2 kW peak, i.e., with a surface of about 5-10 m², combined with limited capacity energy storage (of the order of 1-5 kWh, corresponding to about 1-2 car batteries) and a smart energy management policy, can lead to an effective exploitation of renewable energy.

Index Terms—Radio access network, Base station, Energy consumption, Renewable energy, Green networking, Solar panel

I. INTRODUCTION

Green networking has been a hot research topic for the last 15 years, since the seminal paper by Gupta and Singh [1] raised the awareness of the networking research community on the increasing amount of energy necessary to run the Internet. The attention devoted by researchers to green networking is the result of a multidimensional concern, evolving around three main axes: i) the energy density required to run networks in large metropolitan areas, ii) the carbon footprint of the networking domain, iii) the energy contribution to the operational expenditures (OPEX) of network operators.

A number of international research projects have been devoted to the issue of energy efficiency in networking over the last decade, such as EARTH [2], ECONET [3], TREND [4], and GreenTouch [5]. Many approaches to a more parsimonious use of energy have been developed within those projects, mostly related to the introduction of sleep modes (or low-power-idle modes) in the operation of network equipment (see for example [6]–[8] for a survey of research in the field). At the same time, networking component manufacturers managed to develop new generations of devices with an increased attention to power consumption.

In the particular case of radio access networks (RANs), the most energy-hungry components are base stations (BSs), that largely contribute to the OPEX incurred by mobile network operators (MNOs). Consider for example that China Mobile, the world's largest MNO, with a few million installed BSs, pays an energy bill corresponding to a consumption of several tens TWh per year [9]. While BS models of the last decade consumed up to 3.5 kW, the latest models need less than 1 kW [10].

The expected reduction of the energy intake of BSs spurred investigations of the feasibility of using renewable energy sources (RES), solar radiation in particular, to power BSs in locations where the power grid is not available or not reliable, or just where the cost of connecting the BS to the power grid is high. Exploiting RES means using "green energy" rather than the "brown energy" available from the power grid, which is mostly generated by burning fossil fuels. The results of these studies generally indicate that the area of solar panels that are necessary to power a BS is large [11]; so large to make the solar panel deployment problematic, especially within urban areas.

In this paper, expanding the approach first presented in [12], we use a modeling technique based on Markov reward processes to investigate the possibility of combining small area solar panels and small capacity batteries with a connection to the power grid, aiming at increasing the amount of green energy used to run the BS, and of reducing the MNO OPEX due to energy. Brown energy is drawn from the power grid only when needed to keep the BS running, or during the night, which corresponds to the period with lowest energy consumption, hence with lowest energy price. This has advantages in terms of reduction of both cost and carbon footprint, since the excess energy that is produced in periods of very low consumption may be wasted. The key contributions of this paper are the following:

- We apply a Markov reward model to the investigation of the energy consumption of a BS connected to a solar panel, an energy storage and the power grid. The reward describes the battery charge as a continuous variable, which in previous studies was shown to be the most critical system element as regards quantization [13].
- We investigate the difference in behavior and performance of the BS power system over the 4 seasons by considering a location at 45 degrees North (Torino, Italy), where the impact of seasons is significant.
- We show that small area solar panels (of the order of 1-2 kW peak, i.e., about 5-10 m²) combined with limited capacity energy storage (of the order of 1-5 kWh, corresponding to about 1-2 lead acid, 12 V, 120 Ah, car

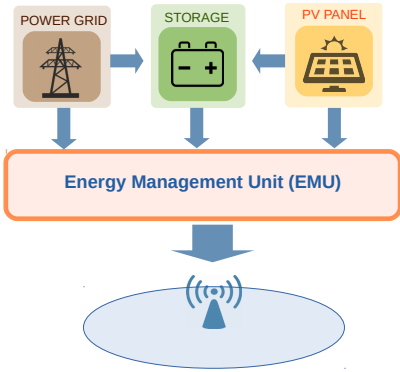


Fig. 1: The considered BS power system.

batteries) and a smart energy management policy, can lead to an effective exploitation of renewable energy. That is, can lead to systems where the overall energy cost (including both capital and operational expenditures) is less than that for a grid-powered BS, and the fraction of used green energy is significant.

The rest of this paper is structured as follows. Section II describes the system setup that we consider in this paper. Section III illustrates the Markov reward model developed for the considered scenario. Section IV presents and discusses numerical results. Section V describes some previous work related to the content of this paper, and Section VI concludes the paper.

II. SYSTEM DESCRIPTION

We consider one macro BS, equipped with a solar panel and an energy storage unit. The BS power system is controlled by an energy management unit (EMU) that is connected to the BS, the solar panel, the energy storage (that we will simply call “battery”) and the power grid. The considered setup is illustrated in Fig. 1.

During periods of energy production of the solar panel, the EMU uses the generated power to run the BS. If the generated power is less than necessary, power is drained from the battery. If the generated power is more than necessary, the excess power is directed to the battery. If the power generated by the panel is insufficient to run the BS and the battery is depleted, power is acquired from the grid.

Power can also be drawn from the grid in periods of low energy cost to recharge the battery for later use. Moreover, the energy entering and exiting the battery is subject to losses, that we assume equal to 15% at both the battery input and output.

A. Energy consumption model

In order to model the BS power consumption we use the approach that has become standard in the field, and that was defined in the FP7 project EARTH [2]. The power needed to operate a macro BS can be expressed as:

$$P_{in} = N_{TX} \cdot (P_0 + \Delta_p \cdot P_{out}), \quad 0 < P_{out} < P_{max} \quad (1)$$

where N_{TX} is the number of BS transceivers, P_{max} represents the maximum radio frequency output power at full load for one transceiver, P_0 corresponds to the fixed power consumption for one transceiver when the radio frequency output power is zero, and Δ_p is the slope of the load-dependent power consumption. P_{out} is derived as:

$$P_{out} = \rho \cdot P_{max}, \quad 0 \leq \rho \leq 1 \quad (2)$$

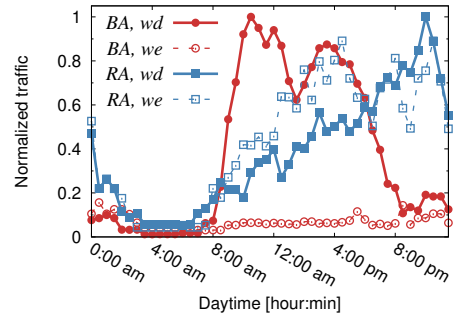


Fig. 2: Week-day (wd) and week-end (we) traffic loads in a business (BA) and residential (RA) area.

where ρ denotes the instantaneous normalized BS load.

The power consumption of a LTE macro BS with 3 sectors, 2x2 MIMO, operating over 20 MHz has been derived as in [10], according to which the typical minimum and maximum values of the power consumption P_{in} are 114.5 W and 817.1 W, respectively.

The daily variation of the parameter ρ is defined by the BS traffic profiles. We use real traces provided by an Italian mobile network operator [13]. The daily traffic patterns measured in a cell in a business area (BA) and in a cell in a residential area (RA), during week-day (wd) and week-end (we), are provided in Fig. 2, setting the maximum observed load equal to the maximum load that can be carried by the BS (i.e., $\rho = 1$).

B. Renewable energy production model

The parameters of the energy production stochastic model are derived from two traces available in the Solar Radiation Data (SoDa) website for the city of Torino, Italy [14]. The first (long-term) trace contains daily average irradiance values, collected from January 1st 1985 to December 31st 2005. The second (short-term) trace contains hourly average irradiance values, collected from February 1st 2004 to December 31st 2006. This data is provided by NASA (USA) and MINES Paris Tech/Armines (France), considering global radiation in the horizontal plane.

We aggregate the available long-term and short-term data into 4 season-based sets: Winter months, from December to February (90 or 91 days per year); Spring, from March to May (92 days); Summer, from June to August (92 days); Autumn, from September to November (91 days). For each season, from the long-term irradiance data we generate the average daily energy production of a 1 kW peak (kWp) solar panel, and we define an energy production histogram by applying an equal-range discretization. That is, we first divide the total production range (difference between the maximum and minimum daily average productions over the 21-year period in the considered season) into 5 ranges of equal size, as in [13], and we compute the frequency (probability) of each interval. This procedure defines *day-types*, i.e., distinguishes between 5 types of days based on the average daily production. The same data are also used to obtain the probabilities that a day-type j follows a day-type i , with $i, j \in [1, \dots, 5]$.

Given the day-type, using the short-term irradiance data we also model the hourly energy production. We split the energy produced at a given hour of a given day-type into ranges of 100 Wh each, and we build a histogram for all samples of a given day-type in a given season. The number of possible intervals of size 100 Wh varies according to season

and it is denoted by $N_L^{(S)}$ for season S , so that the maximum production in season S is $100 \cdot N_L^{(S)}$ Wh.

Fig. 3 reports the average hourly irradiance profiles for each season. As expected, irradiance is highest in summer and lowest in winter, and values of irradiance in spring are significantly higher than in autumn. Note also the difference among useful irradiance hours in the different seasons; while in summer irradiance values are higher than zero from about 5 am to 9 pm, in winter the useful interval is from 7 am to 6 pm. The average daily peaks vary from 333 W/m^2 in winter to 791 W/m^2 in summer. In Fig. 4, instead, we disaggregate the seasonal data, and we report for summer and winter the average irradiance profiles observed for each day-type. The figure shows the importance not only of distinguishing the seasons but also of modeling differences among days of the same season.

Fig. 5 further disaggregates the irradiance data and displays the daily irradiance profiles observed for each day-type in summer and winter. We can see that in summer, day-type 5 corresponds to patterns of high irradiance values, with limited variability from day to day. For day-types corresponding to intermediate to low solar irradiance, a higher variability from day to day can be observed, as well as a more relevant intra-day variation. For day-type 1 we can note a limited variability in irradiance in winter but a very high variability in summer.

These intra-day variabilities for a fixed day-type suggest that a careful description of the renewable energy production process must account not only for the day-type and the hour of the day, but also for the possibility of variations in irradiance within the day-type at a given hour. The histograms for the different day-types in winter and summer are reported in Fig. 6, and examples of histograms for specific time slots, which refer to 12 noon in winter and summer, are reported in Fig. 7. These histograms provide the probabilities that a given amount of energy is generated at noon in winter and summer (similar histograms provide the equivalent data for other times, as well as for spring and autumn) in the various day-types.

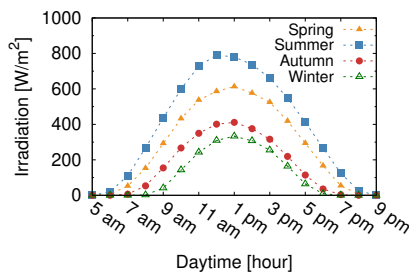


Fig. 3: Average daily irradiance per season.

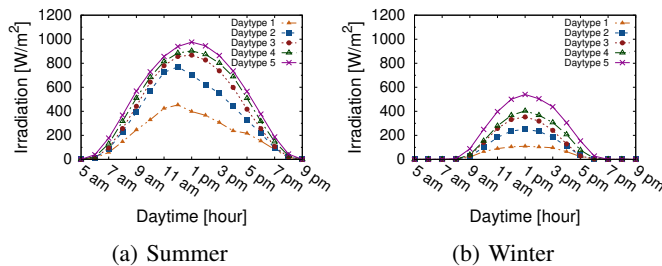


Fig. 4: Average daytype profiles of solar irradiance in summer and winter.

III. MARKOV REWARD MODEL

We define a discrete-time Markov chain (DTMC) reward model for each season S , $\mathcal{Z}^{(S)} = \{\bar{z}_n^{(S)} : n = 0, 1, \dots\}$, over time slots of duration ΔT , set to 1 h in accordance to the time granularity of our data about solar irradiance and traffic and to the findings in [13]. For ease of notation, in what follows we focus on the description of the DTMC for a given season, and we drop the index S . However, even if not explicitly indicated, the model parameter values depend on season. The DTMC state is defined by three variables:

$$\bar{z}_n = (W_n, T_n, L_n),$$

where W_n indicates the day-type at step n ; T_n represents the time of the day at step n , and L_n corresponds to the level of solar irradiance at time T_n . The battery charge level is captured by an accumulated reward random variable, namely B_n at step n . Roughly speaking, in each state the reward varies according to the amount of energy drained from or stored in the battery. This amount depends on the produced energy that is a random variable that, in its turn, depends on the state \bar{z}_n .

The DTMC moves from state $\bar{z}_n = (W_n, T_n, L_n)$ to state $\bar{z}_{n+1} = (W_{n+1}, T_{n+1}, L_{n+1})$ according to the following rules.

Flow of time: The daily evolution of the system is organized into 24 slots, corresponding to the hours of a day:

$$T_{n+1} = (T_n + 1) \bmod 24. \quad (3)$$

Day-type variation: The day-type changes at the end of the day according to the probabilities derived from the long-term data about the daily irradiance, as described in Section II:

$$W_{n+1} = \begin{cases} W_n & \text{with pr. 1} & \text{if } 0 \leq T < 23 \\ W_{n+1} & \text{with pr. } P\{W_{n+1}|W_n\} & \text{if } T = 23, \end{cases} \quad (4)$$

where $P\{W_{n+1}|W_n\}$ is the probability that after a day of type W_n a day of type W_{n+1} follows, computed as described in the previous section.

Irradiance: The probability that the irradiance is equal to one of the possible values of L_n depends on the day-type W_n and the time of the day T_n , according to the statistics obtained from the short-term irradiance:

$$L_n = f(W_n, T_n). \quad (5)$$

This means that including L_n in the DTMC state definition is not necessary, but convenient for the computation of rewards.

Finally, the battery charge level is a continuous random variable represented by the accumulated reward. The reward gained when the DTMC visits state \bar{z}_n is $r(\bar{z}_n)$ and its value depends on three variables:

- $E(\bar{z}_n)$: the amount of energy that is produced by the PV panel in state \bar{z}_n . This amount depends only on the panel size and on L_n and it is given by αL_n , where α is a constant that describes the efficiency of the PV panel;
- $C(\bar{z}_n)$: the amount of energy that is consumed by the BS in state \bar{z}_n , which depends only on the time of the day T_n and on the considered traffic profile (residential or business);
- $A(\bar{z}_n)$: the amount of energy that is acquired from the power grid in state \bar{z}_n . This amount depends on the energy purchasing policy.

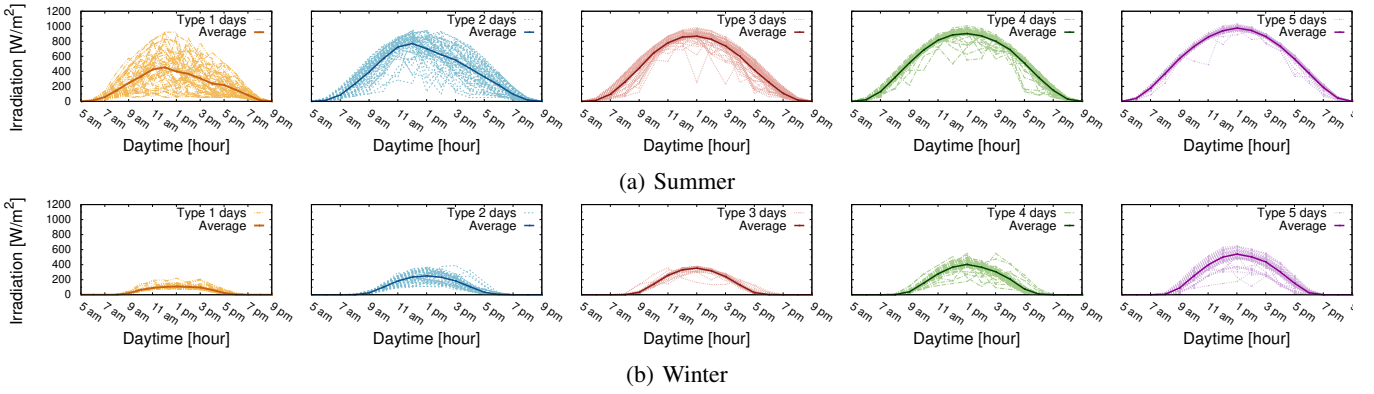


Fig. 5: Daily profiles of solar irradiance in summer and winter.

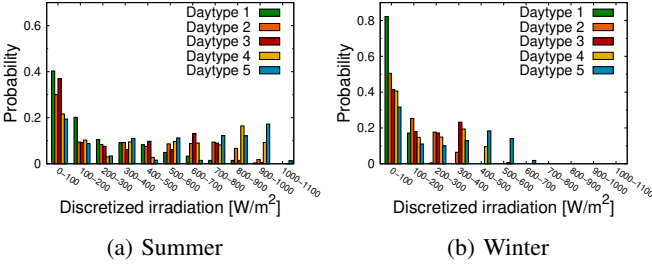


Fig. 6: Probability density function of solar irradiance in summer and winter.

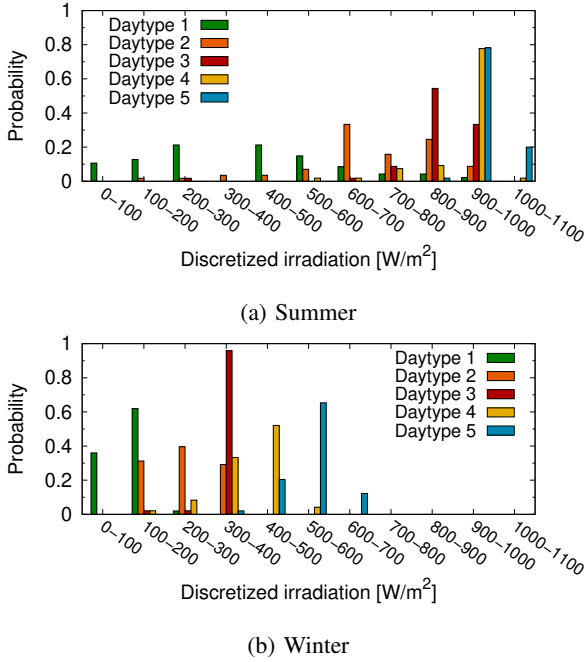


Fig. 7: Probability density function of solar irradiance at 12 noon in Summer and Winter.

Then, the reward $r(\bar{z}_n)$ is expressed as:

$$r(\bar{z}_n) = E(\bar{z}_n) - C(\bar{z}_n) + A(\bar{z}_n). \quad (6)$$

The battery charging and discharging process is captured by the evolution of the cumulative reward B , given by:

$$B_{n+1} = \begin{cases} 0, & \text{if } B_n + r(\bar{z}_n) \leq 0 \\ B_{\max}, & \text{if } B_n + r(\bar{z}_n) \geq B_{\max} \\ B_n + r(\bar{z}_n), & \text{otherwise} \end{cases} \quad (7)$$

where we account for the fact that the battery charge cannot be negative, and cannot exceed the battery capacity B_{\max} .

A. Reward Model Solution

The system model we just described belongs to the class of Markov-modulated fluid flow models with finite buffer, for which a variety of methods have been derived to obtain the buffer occupancy steady-state distribution. Classical numerical solution methods rely on solving partial differential equations (see for instance, [15]). A different set of solution approaches, developed by Ramaswami and his colleagues [16], [17], is based on the observation that the steady-state distribution of Markovian fluid flow models can be obtained from a quasi birth and death (QBD) queue. The connection to a QBD reduces the solution of a fluid model to the analysis of a discrete-time, discrete-state space QBD for which well-tested stable algorithms exist that avoid the computational difficulties arising in spectral methods. In this work, we apply the numerical method presented in [17], since we deal with the steady-state analysis of the charge in a finite-capacity battery¹.

In a nutshell, the numerical solution method introduced by Ramaswami et al. in [17] creates coupled queues on a common probability space, by using a sequence of “spatial uniformizations”, rather than the usual “time uniformization” technique [18]. The main idea of the approach is to define a discretization of the time axis, through a Markovian point process such that, in the inter-event intervals of that process, the potential increments to the flow process are identically distributed exponential random variables. Then, the fluid level is approximated by a number of exponentially distributed chunks, and a queuing model that can be represented with a QBD process is obtained. By letting the parameter of the uniformization process define progressively finer discretizations, the fluid process is obtained as the stochastic process limit of the work in the queues generated in the solution. Once the original fluid process is “reduced” to a QBD process, matrix-geometric analysis can be applied to characterize the steady-state characteristics of the fluid flow process. We refer the interested reader to the original paper [17] to get further details about the numerical method.

B. Energy Management Policies

With the model described above we can represent different energy management policies. We consider the following cases. **Only-battery policy.** Brown energy is acquired only when green energy is not available to run the BS, from either the PV panel or the battery. The amount of energy acquired

¹The implementation of the method was kindly provided to the authors by V. Ramaswami.

from the power grid, $A(\bar{z}_n)$, used in (6), when nonzero, is given by:

$$A(\bar{z}_n) = \begin{cases} C(\bar{z}_n) - E(\bar{z}_n) - B_{n-1} & \text{if } C(\bar{z}_n) - E(\bar{z}_n) - B_{n-1} > 0 \\ & \text{for } 0 \leq T_n \leq 23 \end{cases}$$

Night-consumption policy. Brown energy is acquired from the grid, in the interval from midnight to 6 am, in a quantity equal to what necessary to run the base station, so that no energy is drained from the battery in this period. Note that in this period energy prices are lowest. Moreover, brown energy is acquired also in other periods of the day whenever green energy is not available to run the BS, from either the PV panel or the battery:

$$A(\bar{z}_n) = \begin{cases} C(\bar{z}_n) - E(\bar{z}_n) - B_{n-1} & \text{if } C(\bar{z}_n) - E(\bar{z}_n) - B_{n-1} > 0 \\ & \text{and if } 7 \leq T_n \leq 23 \\ C(\bar{z}_n) & \text{if } 0 \leq T_n \leq 6 \end{cases}$$

Night-consumption-and-recharge policy. Brown energy is acquired from the grid, in the interval from midnight to 6 am, in a quantity equal to what necessary to run the base station plus an additional amount, denoted M , of either 1 kWh per hour (version 1), so that in this period the battery level grows of 7 kWh, or 0.5 kWh per hour (version 2), so that in this period the battery level grows of 3.5 kWh. As before, brown energy is acquired also in other periods of the day when green energy is not available to run the BS, from either the PV panel or the battery:

$$A(\bar{z}_n) = \begin{cases} C(\bar{z}_n) - E(\bar{z}_n) - B_{n-1} & \text{if } C(\bar{z}_n) - E(\bar{z}_n) - B_{n-1} > 0 \\ & \text{and if } 7 \leq T_n \leq 23 \\ C(\bar{z}_n) + M & \text{if } 0 \leq T_n \leq 6 \end{cases}$$

When the acquired energy fills the battery, the value of the reward representing the battery charge will reach B_{\max} as indicated in (7).

C. Performance Measures

From the steady-state distribution of the DTMC reward model for a given season S , with the steady-state probability to be in state \bar{z} denoted by $\pi^{(S)}(\bar{z})$, we can evaluate a set of useful performance metrics:

- $P_e^{(S)}$, the empty battery probability in season S :

$$P_e^{(S)} = \sum_{\forall W} \sum_{\forall T} \sum_{\forall L} P[B = 0 | \bar{z} = (W, T, L)] \pi^{(S)}(\bar{z}).$$

When the battery is empty and no energy is produced, some brown energy has to be taken from the grid to power the BS.

- $E[Q^{(S)}]$, the hourly average amount of energy purchased from the power grid under the only-battery and the night-consumption policies, in season S :

$$E[Q^{(S)}] = \sum_{\forall W} \sum_{\forall T} \sum_{\forall L} A(W, T, L) \pi^{(S)}(W, T, L).$$

In the night-consumption-and-recharge policy, during the night hours, to account for the possibility that the extra-energy M is not acquired because the battery is full,

the component M of the reward $A(W, T, L)$ is summed only if the battery is not full:

$$E[Q^{(S)}] = \sum_{\forall W} \sum_{\forall T} \sum_{\forall L} [C(W, T, L) + M(1 - P_f(W, T, L))] \pi^{(S)}(W, T, L)$$

where $P_f(W, T, L)$ is the probability that, in state (W, T, L) , the battery is full.

- $E[X^{(S)}]$, the hourly average cost of the energy purchased from the power grid under the only-battery and the night-consumption policies, in season S :

$$E[X^{(S)}] = \sum_{\forall W} \sum_{\forall T} P^{(S)}(T) \sum_{\forall L} A(W, T, L) \pi^{(S)}(W, T, L),$$

where $P^{(S)}(T)$ is the electricity price, which depends on the season and on the time of the day T . Like for the amount of purchased energy, also for the evaluation of the cost, under the night-consumption-and-recharge policy, we need to take into account that the extra-energy M is purchased only if the battery is not full:

$$E[X^{(S)}] = \sum_{\forall W} \sum_{\forall T} P^{(S)}(T) \sum_{\forall L} [C(W, T, L) + M(1 - P_f(W, T, L))] \pi^{(S)}(W, T, L)$$

- E_G , the yearly energy purchased from the grid:

$$E_G = 24 \sum_{\forall S} E[Q^{(S)}] D^{(S)},$$

where $D^{(S)}$ is the total number of days in a given season S .

- C_G , the yearly OPEX due the purchased brown energy:

$$C_G = 24 \sum_{\forall S} E[X^{(S)}] D^{(S)}.$$

Moreover, the yearly CAPEX of PV panels, denoted by C_{PV} , and the CAPEX resulting of the battery usage, denoted by C_B , are defined as:

$$C_{PV} = \frac{c_P S_{PV}}{l_P} \quad (8)$$

$$C_B = \frac{c_B S_B}{l_B}, \quad (9)$$

where c_P is the cost for 1 kWp of PV panel capacity, S_{PV} is the PV panel capacity, c_B is the cost for 1 kWh lead-acid battery capacity, S_B is the battery capacity, l_P is the lifecycle of a PV panel (in years) and l_B is the expected lifespan of the set of batteries (in years).

Finally, the green-to-brown energy ratio, denoted by GB , is defined as:

$$GB = \frac{E_{BS} - E_G}{E_G}, \quad (10)$$

where E_{BS} is the yearly BS energy consumption.

IV. NUMERICAL RESULTS

As already mentioned, we consider one macro BS with 2 transceivers, adopting the BS models of [10] with the corresponding energy consumption. We consider the traffic profiles presented in Fig. 2, focusing on the residential weekday version, which was shown in [12] to be more critical due to the temporal mismatch between energy production peak and traffic peak. Recall that we assume energy losses of 15% at both the battery input and output.

Moreover, we consider three values for the PV panel size: 1, 2 and 5 kWp, and three battery capacities: 1, 2 and 5 kWh. As already noted, these PV panel sizes correspond to about 5, 10, and 25 square meters, and the battery capacities correspond to about 1 or 2 car batteries (considering 12 V, 120 Ah, lead-acid batteries).

An ideal system configuration should yield small empty battery probability, so that little brown energy must be acquired from the grid, and a full battery probability not too close to 1, in order to avoid wasting the green energy produced by the PV panel. In our previous work [12], results showed that, as expected, for growing PV panel size, the probability that the battery is empty decreases, while the probability that the battery is full grows. The best choice of the PV panel size is however quite dependent on the solar irradiance levels, hence on the season. This led to the suggestion of adopting different approaches to energy management in the different seasons.

However, the real driver to convince a network operator to adopt renewable energy to power base stations must be based on the possibility of a reduction in the total cost to power the base station, including both capital and operational expenditures (CAPEX and OPEX), combined with a significant reduction of the carbon footprint, that today can represent a competitive advantage in the attraction of customers. In Fig. 8 we show for the four considered energy management policies, the three PV panel sizes, and the three battery sizes, the total amount of energy bought from the grid, the yearly CAPEX due to the PV panel (assuming a panel duration of 25 years and a cost of 660 €/kWp), the yearly CAPEX due to storage (assuming a 100 €/kWh lead-acid battery cost and a maximum of 3000 discharge cycles before replacement [19]), the cost of the energy bought from the grid (assuming real prices from the Italian electricity market provided by GME [20]), and the total cost to power the base station. We can see that (small) cost reductions can only be obtained with PV panel sizes equal to either 1 or 2 kWp, and battery sizes equal to 1 or 2 kWh, and only with the Only-battery and Night-consumption energy management policies. The adoption of different energy management policies in different seasons yields small additional cost savings (not shown in the plots) with small PV panel sizes only. For example, with 1 kWp panel size and 2 kWh battery, the additional saving is about 2.5%; increasing the battery size to 5 kWh brings the additional saving to almost 6%. Larger sizes of battery (above 10 kWh) yield overall CAPEX and OPEX costs higher than the cost of BSs systems powered only by the electrical grid.

This is quite an interesting result, since it proves that small solar systems, including a PV panel of limited size and a small battery, which are easily deployable also in urban environments, can help the operator reduce costs, while also allowing a reduction of the RAN carbon footprint.

The question about the effectiveness of such small systems in reducing the carbon footprint of the base station is answered by the results in Fig. 9, which plots the ratio between the amounts of green and brown energy used to power the base station. Results show that the cases that yield a cost reduction, and in which the ratio is close to 1 are those with battery capacity of 2 kWh and PV panel sizes of 2 kWp. This means a reduction of 50% of the brown energy consumed by the base station, with the associated reduction of its carbon footprint, using manageable size PV panels and

batteries, and decreasing the overall cost with respect to the traditional connection to the power grid.

It must be noted that the results in Fig. 9 also show that larger battery capacities yield further reductions of the carbon footprint, but, as we already noted, do not allow a reduction of the overall cost.

V. RELATED WORK

The increasing number and variety of works available in the literature about green mobile networks shows the raising interest about the use of RE to make communication networks more energy efficient [21]–[23].

Most related with this paper are the works that aim at modeling the behavior of BS power systems based on renewables, with the objective of understanding the characteristics of these systems and providing guidelines for correct dimensioning [13], [24]–[26]. Those works rely on Markovian models for computing BSs performance, in which battery charge levels are explicitly modeled as one of the Markov chain state-variables. To the best of our knowledge, our works are the first that apply Markov reward models for dimensioning both panel and battery sizes of BS renewable power systems. Applying reward technique to describe the battery charge as a continuous variable enables a more accurate performance evaluation of a BS system, given that previous studies showed that battery modeling is the most critical system element as regards quantization [13].

VI. CONCLUSIONS

In this paper we considered a base station that, besides being connected to the power grid, is equipped with a solar panel and an energy storage unit, with the objective of reducing both the total cost of the base station power system, and the base station carbon footprint.

By modeling the system as a Markov reward process, we investigated three energy management strategies: i) brown energy is drained from the grid only when the battery is empty, ii) the base station is powered through brown energy from the grid also during night, when the price of electricity is low, and, iii) during night, in addition to the energy needed to run the BS, some brown energy is proactively stored in the battery for future use.

Results show that some (admittedly small) overall cost saving, together with significant (of the order of 50%) carbon footprint reductions can be obtained with PV panel sizes of the order of 10 square meters and 1 or 2 car batteries for energy storage. This makes the adoption of mixed base station power system, composed of a connection to the grid, a solar panel and a battery, feasible in a large number of scenarios, including urban environments, where network densification will soon call for the deployment of many new base stations.

REFERENCES

- [1] M. Gupta and S. Singh, "Greening of the internet," in *Proceedings of SIGCOMM 2003*.
- [2] D. Zeller, M. Olsson, O. Blume, A. Fehske, D. Ferling, W. Tomaselli, and I. Gódor, *Sustainable Wireless Broadband Access to the Future Internet - The EARTH Project*. Springer Berlin Heidelberg, 2013.
- [3] R. Bolla, R. Bruschi, F. Davoli, L. D. Gregorio, L. Giacomello, C. Lombardo, G. Parladori, N. Strugo, and A. Zafeiropoulos, "The low energy consumption networks (econet) project," in *2nd IFIP Conf. on Sustainable Internet and ICT for Sustainability*, 2012.
- [4] M. Ajmone Marsan, C. Guerrero, S. Buzzi, F. Idzikowski, L. Chiaraviglio, M. Meo, Y. Ye, and J. L. Vizcaíno, "TREND: toward real energy-efficient network design," in *2nd IFIP Conf. on Sustainable Internet and ICT for Sustainability*, 2012.

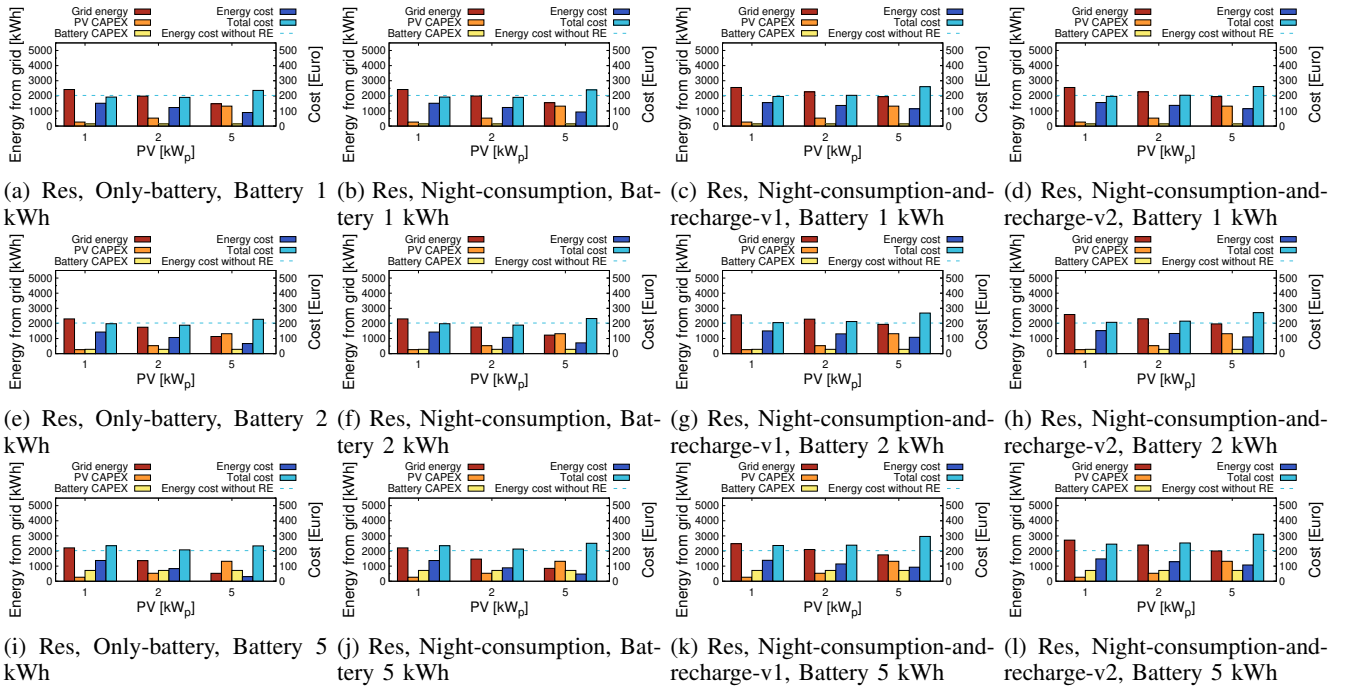


Fig. 8: Energy bought from the grid per year and yearly CAPEX/OPEX in residential areas for different battery and PV panel sizes, and for different energy management policies

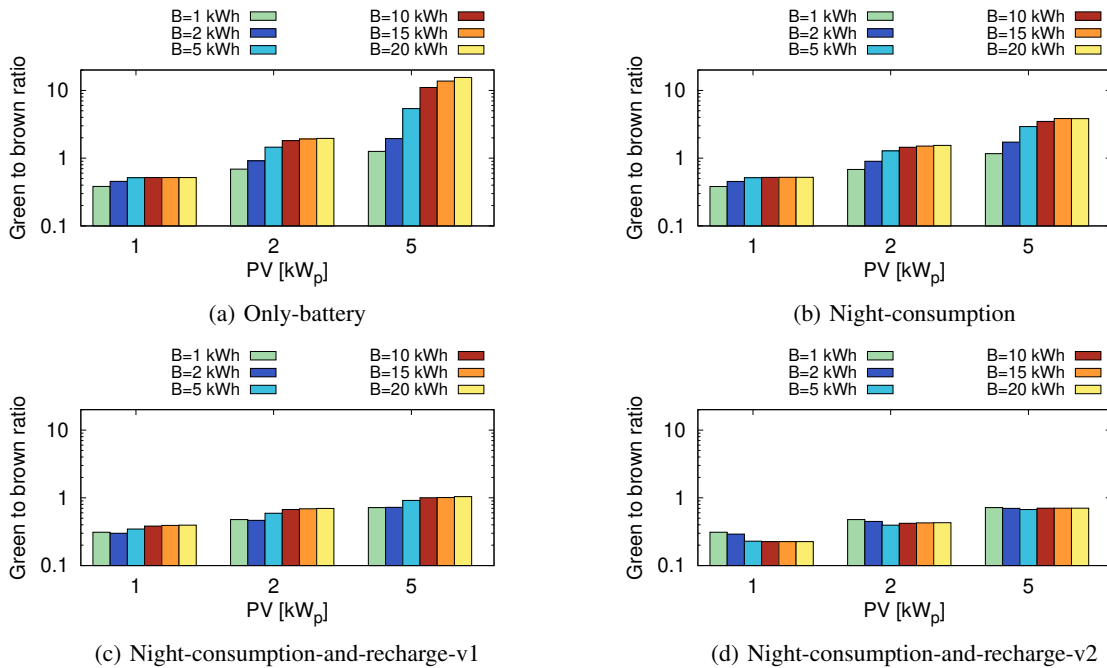


Fig. 9: Green/Brown energy ratio in residential areas for different battery and PV panel sizes, and for different energy management policies

- [5] GreenTouch Consortium, 2015. [Online]. Available: <https://s3-us-west-2.amazonaws.com/belllabs-microsite-greentouch/index.php?page=about-us.html>
- [6] Z. Hasan, H. Boostanimehr, and V. K. Bhargava, "Green cellular networks: A survey, some research issues and challenges," *Communications Surveys & Tutorials, IEEE*, vol. 13, pp. 524 – 540, 2011.
- [7] A. D. Domenico, E. C. Strinati, and A. Capone, "Enabling green cellular networks: A survey and outlook," *Computer Communications*, vol. 37, pp. 5 – 24, 2014.
- [8] L. Budzisz, F. Ganji, G. Rizzo, M. A. Marsan, M. Meo, Y. Zhang, R. Tassiulas, S. Lambert, B. Lannoo, M. Pickavet, A. Conte, I. Haratcherev, and A. Wolisz, "Dynamic resource provisioning for energy efficiency in wireless access networks: A survey and an outlook," *IEEE Communications Surveys & Tutorials*, pp. 2259–2285, 2014.
- [9] Disclosure Inside Act, 2010. [Online]. Available: <https://www.cdp.net/zh/articles/climate/case-study-china-mobile>
- [10] B. Debaillie, C. Desset, and F. Louagie, "A flexible and future-proof power model for cellular base stations," in *81st IEEE Vehicular Technology Conference*, 2015.
- [11] M. Meo, Y. Zhang, R. Gerboni, and M. Ajmone Marsan, "Dimensioning the power supply of a LTE macro BS connected to a PV panel and the power grid," in *IEEE International Conference on Communications*, 2015.
- [12] A. P. Couto da Silva, D. Renga, M. Meo, and M. Ajmone Marsan, "Small solar panels can drastically reduce the carbon footprint of radio access networks," in *31st International Teletraffic Congress*, 2019.
- [13] A. P. Couto da Silva, D. Renga, M. Meo, and M. Ajmone Marsan, "The impact of quantization on the design of solar power systems for cellular base stations," *IEEE Transactions on Green Communications and Networking*, vol. 2, no. 1, pp. 260–274, 2018.

- [14] SODA (Solar radiation Data), “Solar Energy Services for Professionals,” 2014. [Online]. Available: <http://www.soda-pro.com/>
- [15] D. Anick, D. Mitra, and M. Mohan Sondhi, “Stochastic theory of a data-handling system with multiple sources,” *Bell System Technical Journal*, vol. 61, 1982.
- [16] S. Ahn and V. Ramaswami, “Fluid flow models and queues: A connection by stochastic coupling,” *Stochastic Models*, vol. 19, 2003.
- [17] —, “Steady State Analysis of Finite Fluid Flow Models Using Finit QBDs,” *Queueing Systems*, no. 49, pp. 223–259, 2005.
- [18] A. Jensen, “Markoff chains as an aid in the study of markoff processes,” *Skandinavisk Aktuarietidskrift*, vol. 36, pp. 87–91, 1953.
- [19] “Joint EASE-EERA Recommendations for a European Energy Storage Technology Development Roadmap Towards 2030,” 2017.
- [20] “Gestore Mercati Energetici - 2018 Day Ahead Market prices (MGP),” <https://www.mercatoelettrico.org/En/Default.aspx>.
- [21] D. Renga, H. A. H. Hassan, M. Meo, and L. Nuaymi, “Improving the interaction of a green mobile network with the smart grid,” in *IEEE International Conference on Communications*, 2017.
- [22] M. Ali, M. Meo, and D. Renga, *Cost Saving and Ancillary Service Provisioning in Green Mobile Networks: Technology, Communications and Computing*. Springer, 2019, pp. 201–224.
- [23] M. H. Alsharif, J. Kim, and J. H. Kim, “Green and sustainable cellular base stations: An overview and future research directions,” *Energies*, vol. 10, no. 5, 2017.
- [24] V. Chamola and B. Sikdar, “Outage estimation for solar powered cellular base stations,” in *IEEE International Conference on Communications*, 2015.
- [25] J. Song, V. Krishnamurthy, A. Kwasinski, and R. Sharma, “Development of a markov-chain-based energy storage model for power supply availability assessment of photovoltaic generation plants,” *IEEE Transactions on Sustainable Energy*, vol. 4, no. 2, pp. 491–500, 2013.
- [26] G. Leonardi, M. Meo, and M. A. Marsan, “Markovian models of solar power supply for a LTE macro BS,” in *IEEE International Conference on Communications*, 2016.